Electromagnetically induced transparency in ladder-type inhomogeneously broadened media: Theory and experiment

Julio Gea-Banacloche, Yong-qing Li, Shao-zheng Jin, and Min Xiao
Department of Physics, University of Arkansas, Fayetteville, Arkansas 72701
(Received 10 May 1994)

We develop a theory of electromagnetically induced transparency in a three-level, ladder-type Doppler-broadened medium, paying special attention to the case where the coupling and probe beams are counterpropagating and have similar frequencies, so as to reduce the total Doppler width of the two-photon process. The theory is easily generalized to deal with the Λ configuration, where the ideal arrangement involves two copropagating beams. We discuss different possible regimes, depending on the relative importance of the various broadening mechanisms, and identify ways to optimize the absorption-reduction effect. The theory is compared to the results of a recent experiment (on a ladder-type system), using the Rb $D2$ line, with generally very good agreement. The maximum absorption reduction observed (64.4%) appears to be mostly limited by the relatively large (~5 MHz) linewidth of the diode lasers used in our experiment.

PACS number(s): 42.50.Hz, 32.80.Wr, 42.65.Ky

I. INTRODUCTION

Electromagnetically induced transparency (EIT) is the effect behind some recent proposals for lasing without inversion [1]. A possible level scheme for EIT is shown in Fig. 1(a). Under normal circumstances, with most of the population in the lower level $|1\rangle$, the probe beam on resonance with the $|1\rangle \rightarrow |2\rangle$ transition would be strongly absorbed. When a strong "coupling beam" resonant with the $|2\rangle \rightarrow |3\rangle$ transition is added, however, absorption of the probe beam can be greatly reduced (although most of the population is still in the ground state). This possibility of controlling the transparency of a medium by using another beam of light may have useful applications in electro-optical devices and nonlinear optics, in addition to the lasing without inversion applications mentioned earlier [2]. Also, systems similar to the one in Fig. 1(a) have been predicted to exhibit unusual dispersive properties which might also lead to useful new devices [3].

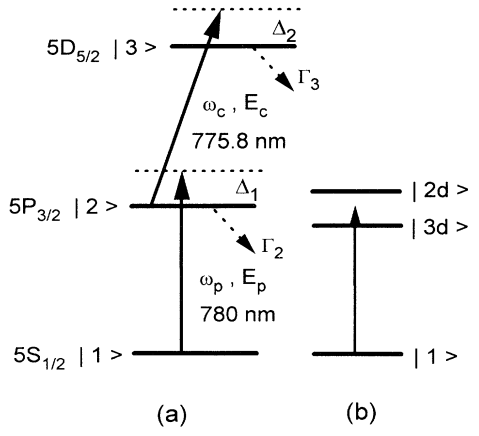

FIG. 1. (a) Relevant energy levels of neutral rubidium atom. (b) Dressed-state picture.

We present here the theory of a recent experiment [4] we carried out on the system of Fig. 1(a) (a gas of rubidium atoms). We believe this experiment to be the first one to observe EIT in an inhomogeneously broadened medium, with cw lasers continuously tunable over a broad range of frequencies [5]. This makes a detailed, quantitative comparison to a relatively simple theory possible and this is one of the main purposes of this article. As regards the theoretical treatment itself, its main new feature is the explicit inclusion of inhomogeneous broadening, which is treated exactly (to lowest order in the weak probe field) so that the influence of the various broadening mechanisms may be assessed in a variety of different regimes and in particular in the "almost Doppler-free" configuration of our experiment. Our formulas for the ladder system can easily be extended to the Λ configuration and we also indicate how to do it here.

Our paper is organized as follows. In Sec. II we present the theoretical results and in Sec. III a discussion of the experiments and detailed comparison to the theoretical predictions. Section IV contains some brief concluding remarks. Section II is further divided into several subsections, dealing with the derivation of the general, analytical results, their generalization to the Λ level scheme, numerical and analytical study of various limits of interest, and a brief summary of the main points.

II. THEORY

A. General results for the ladder system

Consider the three-level system in Fig. 1(a). Let ω_{21} be the frequency of the $|1\rangle \rightarrow |2\rangle$ transition, ω_p the frequency of the probe laser, and $\Delta_1 = \omega_p - \omega_{21}$ its detuning, and similarly let ω_{32} be the frequency of the $|2\rangle \rightarrow |3\rangle$ transition, ω_c the frequency of the "coupling" laser, and $\Delta_2 = \omega_c - \omega_{32}$ its detuning. Using standard semiclassical

 ©1995 The American Physical Society

methods (see, e.g., [6]), we find the following equations of motion for the matrix elements of the atomic density operator:

$$\dot{\rho}_{32}=-(\gamma_{32}-i\Delta_2)\rho_{32}+ig_{32}E_c(\rho_{33}-\rho_{22})+ig_{21}E_p^*\rho_{31}\ , \tag{1a}$$

$$\dot{\rho}_{21}=-(\gamma_{21}-i\Delta_1)\rho_{21}+ig_{21}E_p(\rho_{22}-\rho_{11})-ig_{32}E_c^*\rho_{31}\ , \tag{1b}$$

$$\dot{\rho}_{31}=-[\gamma_{31}-i(\Delta_1+\Delta_2)]\rho_{31}-ig_{32}E_c\rho_{21}+ig_{21}E_p\rho_{32}\ . \tag{1c}$$

The dipole moment matrix elements for the two transitions are $2\hbar g_{21}$ and $2\hbar g_{32}$; we shall take them to be real for simplicity. E_c (E_p) is the amplitude of the coupling (probe) field. If collisional dephasing is negligible, the decay rates are given by $\gamma_{ij}=(\Gamma_i+\Gamma_j)/2$, where Γ_i is the natural decay rate of level $|i\rangle$ (with $\Gamma_1=0$, since level $|1\rangle$ is the ground state). As we shall show below, as long as we are only interested in the solution of system (1) to lowest order in the weak probe field, the equations of motion for the diagonal density-matrix elements ρ_{ii} are actually not needed and our results are, to that order, independent of any assumptions about the various channels through which the different states may get populated or depleted.

A key ingredient of equations (1) is the presence of the matrix element ρ_{31}, which indicates a coherence between the levels $|3\rangle$ and $|1\rangle$ that develops as a result of the coherent driving of the two allowed transitions. At steady state Eq. (1c) yields

$$\rho_{31}=-\frac{ig_{32}E_c}{\gamma_{31}-i(\Delta_1+\Delta_2)}\rho_{21}+\frac{ig_{21}E_p}{\gamma_{31}-i(\Delta_1+\Delta_2)}\rho_{32}$$
$$\simeq-\frac{ig_{32}E_c}{\gamma_{31}-i(\Delta_1+\Delta_2)}\rho_{21}\ . \tag{2}$$

Here we make our first approximation, namely, neglecting the contribution to ρ_{31} from the upper transition dipole amplitude ρ_{32}. The justification is twofold: first, this term is multiplied by the weak probe field E_p, and second, the population in levels 2 and 3 is probably negligible and so should be ρ_{23}. For a probe strong enough to begin to saturate the $|1\rangle\rightarrow|2\rangle$ transition, this approximation may not hold anymore. Using (2) in (1b) and solving for the steady state we get

$$\rho_{21}=\frac{ig_{21}E_p(\rho_{22}-\rho_{11})}{\gamma_{21}-i\Delta_1+\dfrac{\Omega_c^2/4}{\gamma_{31}-i(\Delta_1+\Delta_2)}}$$
$$\simeq-\frac{ig_{21}}{\gamma_{21}-i\Delta_1+\dfrac{\Omega_c^2/4}{\gamma_{31}-i(\Delta_1+\Delta_2)}}E_p\ , \tag{3}$$

where $\Omega_c\equiv 2g_{32}E_c$ (assuming E_c, the field's complex amplitude, to be real) is the Rabi frequency of the coupling field. In (3) we have made our second approximation, namely, neglecting the population ρ_{22} of the middle level (and therefore also that of the upper level), which means $\rho_{22}\simeq\rho_{33}\simeq 0$ and $\rho_{11}\simeq 1$. The complex susceptibility at the probe field frequency is obtained from the polarization

$$P=\tfrac{1}{2}\epsilon_0E_p[\chi(\omega_p)e^{-i\omega_pt}+\text{c.c.}]$$
$$=-2\hbar g_{21}N\rho_{21}e^{-i\omega_pt}+\text{c.c.}\ , \tag{4}$$

where N is the density of atoms. The real and imaginary parts of the susceptibility $\chi=\chi'+i\chi''$ lead to the dispersion and absorption characteristics of the atomic medium in the usual way, i.e., the intensity absorption coefficient is given by $\alpha=\omega_pn_0\chi''/c$ and the dispersion coefficient (real part of the wave vector k) is given by $\beta=\omega_pn_0\chi'/2c$, where n_0 is the background index of refraction (due to far off-resonance transitions). While the results up to this point are well known, as special cases of other treatments (see, in particular, [7]) we have preferred to derive them explicitly to make the paper self-contained and also to point out clearly which assumptions and approximations are or are not necessary for a good description of our experiment.

The above derivation ignores Doppler broadening. A key ingredient in our experimental scheme is that the probe and coupling beams are counterpropagating and their frequencies are very close. An atom moving towards the probe beam with velocity v "sees" its frequency upshifted by an amount ω_pv/c (to lowest order in v/c), while the frequency of the coupling beam is, for the same atom, downshifted by an amount $-\omega_cv/c$. If the number of atoms per unit volume with velocity v is $N(v)dv$, their contribution to the total susceptibility is

$$\chi(v)dv=\frac{4i\hbar g_{21}^2/\epsilon_0}{\gamma_{21}-i\Delta_1-i\dfrac{\omega_p}{c}v+\dfrac{\Omega_c^2/4}{\gamma_{31}-i(\Delta_1+\Delta_2)-i(\omega_p-\omega_c)v/c}}N(v)dv\ , \tag{5}$$

where the detunings Δ_1 and Δ_2 are defined as the nominal detunings for an atom at rest. In our experiment, ω_p is approximately equal to ω_c and hence the two-photon transition is almost Doppler-free. Even so, the small term $(\omega_p-\omega_c)v/c$ in (5) does make a difference. The total polarizability is obtained by integrating (5) over the velocity distribution, which is conventionally taken to be Maxwellian, i.e.,

$$N(v)=\frac{N_0}{u\sqrt{\pi}}e^{-v^2/u^2}dv\ , \tag{6}$$

where $u/\sqrt{2}$ is the root-mean-square atomic velocity. For a purely Doppler-broadened medium, the full width at half maximum of the absorption profile would be given by

$$\Delta\omega_D = \frac{2\omega_p}{c} u\sqrt{\ln 2} \ . \tag{7}$$

If the small term $(\omega_p-\omega_c)v/c$ is neglected in (5), the integral over velocities yields the relatively simple result

$$\chi = \frac{4i\hbar c g_{12}^2 N_0 \sqrt{\pi}}{\epsilon_0 u \omega_p} e^{z^2}(1-\mathrm{erf} z) \tag{8}$$

with the argument

$$z = \frac{c}{u\omega_p}\left[\gamma_{21} - i\Delta_1 + \frac{\Omega_c^2/4}{\gamma_{31}-i(\Delta_1+\Delta_2)}\right] . \tag{9}$$

The error function of complex argument is available in most mathematical function packages (see also [8]). The particular combination of e^{z^2} and erfz appearing in (8) is also called sometimes the plasma dispersion function (see Appendix C of [6]). Some approximations to this result will be discussed later on.

If the Doppler broadening of the two-photon transition is not neglected, Eq. (5) can still be integrated over the velocity distribution (6), but the results are a little more complicated. One needs to calculate the poles of the denominator in (5), as a function of $z=v/u$,

$$z_{1,2} = -\frac{i}{2}\left[\frac{\gamma_{21}-i\Delta_1}{\omega_p u/c} + \frac{\gamma_{31}-i(\Delta_1+\Delta_2)}{(\omega_p-\omega_c)u/c}\right] \pm \frac{i}{2}\left[\left[\frac{\gamma_{21}-i\Delta_1}{\omega_p u/c} - \frac{\gamma_{31}-i(\Delta_1+\Delta_2)}{(\omega_p-\omega_c)u/c}\right]^2 - \frac{\Omega_c^2}{\omega_p(\omega_p-\omega_c)u^2/c^2}\right]^{1/2} . \tag{10}$$

The result is

$$\chi = \frac{2c}{n_0\omega_p}\left[\beta + i\frac{\alpha}{2}\right] = \frac{2i\hbar c g_{21}^2 N_0\sqrt{\pi}}{\epsilon_0 u\omega_p}\{(1-d)s_1 e^{-z_1^2}[1-s_1\mathrm{erf}(iz_1)] + (1+d)s_2 e^{-z_2^2}[1-s_2\mathrm{erf}(iz_2)]\} , \tag{11}$$

where $s_{1,2} = -\mathrm{sgn}[\mathrm{Im}(z_{1,2})]$ and the quantity

$$d = \frac{i}{z_1-z_2}\left[\frac{\gamma_{21}-i\Delta_1}{\omega_p u/c} - \frac{\gamma_{31}-i(\Delta_1+\Delta_2)}{(\omega_p-\omega_c)u/c}\right] \tag{12}$$

has been defined for convenience. This quantity d approaches ± 1 in the limit in which the Doppler shift of the two-photon transition is negligible, i.e., when $\omega_p-\omega_c$ is sufficiently small. Specifically, if $|\omega_p-\omega_c|/\omega_p \ll \gamma_{31}^2/\Omega_c^2$, we have $d\to\pm 1$ [the sign depends on the choice of a branch for the square root in (10)] and the result (8) is recovered from either the z_1 or the z_2 term in (11). Further approximations leading to simplifications of (8) and (11) in special cases will be discussed in Sec. II C.

We note here the existence of at least one earlier theoretical treatment of this system by Hänsch and Toschek [9]. Their main result, Eq. (58) of [9], is, however, derived under some approximations which make it only of limited validity for our purposes. In particular, they keep the strong-coupling field only to second order, whereas we have kept it to all orders (which we need in order to compare with the experimental results; see Fig. 7 below), and they also make the strong Doppler limit approximation, which does not quite apply to our almost Doppler-free case. A consequence of this approximation in [9] is that they in fact predict a vanishing effect for $\omega_c \le \omega_p$, which is clearly not correct; for instance, our Eqs. (8) and (9) show electromagnetically induced transparency to be quite feasible for the simplest case of $\omega_c=\omega_p$ (completely Doppler-free two-photon transition), as will be discussed in detail in Sec. II C (see also Fig. 2 below).

B. The Λ system

One can formally obtain the so-called Λ (or "folded") level configuration from Fig. 1 by taking the coupling level $|3\rangle$ to lie below level $|2\rangle$. This makes the frequency ω_{32} formally negative; the slowly varying term in the interaction Hamiltonian arises then from the "negative frequency" part of the coupling field, that is, the part that goes as $e^{i\omega_c t}$ (this may also be understood by noting that the transition from $|2\rangle$ to $|3\rangle$ now involves the creation, instead of the annihilation, of a photon). Therefore, the role of Δ_2 in the equations in the preceding subsection is now played by $-\omega_c-\omega_{32}=-\omega_c+\omega_{23}=-\Delta_2$, if the detuning is defined in terms of the positive frequency ω_{23} as $\Delta_2=\omega_c-\omega_{23}$. Equation (3) then becomes

$$\rho_{21} = -\frac{ig_{21}}{\gamma_{21}-i\Delta_1+\dfrac{\Omega_c^2/4}{\gamma_{31}-i(\Delta_1-\Delta_2)}} E_p \tag{13}$$

(Λ system, homogeneously broadened case).

It is clear that when the motion of the atoms is considered, the way to stay close to two-photon resonance in this system is to use two *copropagating* beams (so that both frequencies are either upshifted or downshifted). The equivalent of Eq. (5) then reads

$$\chi(v)dv = \frac{4i\hbar g_{21}^2/\epsilon_0}{\gamma_{21}-i\Delta_1-i\dfrac{\omega_p}{c}v+\dfrac{\Omega_c^2/4}{\gamma_{31}-i(\Delta_1-\Delta_2)-i(\omega_p-\omega_c)v/c}} N(v)dv \tag{14}$$

(Λ system, copropagating pump and probe beams). Then, for the two-photon Doppler-free case ($\omega_c=\omega_p$), the total susceptibility is given by Eq. (8), only with

$$z=\frac{c}{u\omega_p}\left[\gamma_{21}-i\Delta_1+\frac{\Omega_c^2/4}{\gamma_{31}-i(\Delta_1-\Delta_2)}\right] \tag{15}$$

instead of (9), whereas the general case is given by Eq. (11) with

$$\Delta_2\rightarrow-\Delta_2 \tag{16}$$

in Eqs. (10) and (12). Whereas most of the discussions in the following subsection will assume the ladder configuration of our experiment, they all can easily be applied to the Λ system with copropagating beams through the substitution (16) above.

C. Various limits

Although this does not quite apply to our experiment, consider first, for simplicity, what happens if the Doppler broadening of the two-photon transition is ignored altogether because of the counterpropagating pump-probe beam arrangement and the closeness of the two frequencies. Then we obtain Eq. (8). An asymptotic result valid for large $|z|$ (and $|\arg z|<3\pi/4$; see [8]) is

$$e^{z^2}(1-\mathrm{erf}z)\simeq\frac{1}{\sqrt{\pi}}\left[\frac{1}{z}-\frac{1}{2z^3}+\cdots\right]. \tag{17}$$

The argument z given by (9) will be large under two-photon resonance conditions ($\Delta_1=-\Delta_2$) provided that $c\Omega_c^2/4u\omega_p\gamma_{31}\gg1$ or, in terms of the full Doppler width (7), if

$$\frac{\Omega_c^2}{\gamma_{31}\Delta\omega_D}\gg1\ . \tag{18}$$

Equation (18) may hold either for a large Ω_c or a small γ_{31}. If (18) holds and $|\Delta_1+\Delta_2|<\gamma_{31}$, use of (17) in (8) yields the homogeneously broadened result

$$\chi=\frac{4i\hbar g_{12}^2N_0/\epsilon_0}{\gamma_{21}-i\Delta_1+\dfrac{\Omega_c^2/4}{\gamma_{31}-i(\Delta_1+\Delta_2)}}\ . \tag{19}$$

At line center, and for a perfectly tuned coupling beam ($\Delta_2=\Delta_1=0$), the absorption coefficient α is reduced by a factor

$$\frac{\alpha(\Omega_c)}{\alpha(0)}=\left[\frac{1}{\sqrt{\pi}z_0e^{z_0^2}(1-\mathrm{erf}z_0)}\right]\frac{1}{1+\Omega_c^2/4\gamma_{21}\gamma_{31}}\ , \tag{20}$$

where $z_0=c\gamma_{21}/u\omega_p=2\sqrt{\ln2}(\gamma_{21}/\Delta\omega_D)$. In the limit $\gamma_{31}\rightarrow0$, Eq. (18) obviously holds for any value of Ω_c and (20) equals zero (total absorption suppression, perfect transparency).

The assumption $\gamma_{31}\rightarrow0$ (which requires an infinitely long-lived coupling level $|3\rangle$) was made implicitly by Imamoğlu and Harris in [1]. It was shown later by Fleischhauer *et al.* [7] that only under this condition do the atomic evolution equations for the driven Λ or cascade systems reduce to the equations for interference between excited states decaying to the same continuum, originally proposed by Imamoğlu [10] as an example of a system that may show a perfect zero in absorption, but not in emission.

In practice, one will never have $\gamma_{31}=0$, but clearly a large reduction in absorption will take place if (18) holds and

$$\frac{\Omega_c^2}{4\gamma_{21}\gamma_{31}}\gg1\ . \tag{21}$$

For a Doppler-broadened medium ($\Delta\omega_D>\gamma_{21}$), (18) is the more restrictive condition. The assistance provided by the coupling to the third level is, however, immediately apparent. If one had to rely solely on the dynamic Stark shift (equal to $\Omega_c/2$) for the absorption suppression at line center, one would naively expect that values of Ω_c in excess of the $|1\rangle\rightarrow|2\rangle$ transition's natural linewidth γ_{21}, or even the full Doppler linewidth $\Delta\omega_D$, might be necessary in order to see a substantial effect. Instead, by mixing level $|2\rangle$ with the long-lived level $|3\rangle$, one gains a large enhancement factor Ω_c/γ_{31}, so that (18) and (21) may hold even for values of the Rabi frequency much smaller than the Doppler width. In our experiment, $\Omega_c/\Delta\omega_D$ is typically of the order of $\frac{1}{5}$; yet the large value of Ω_c/γ_{31} (of the order of 200) allows us to see a substantial reduction of the absorption at line center.

It remains to be considered what happens when the (small) Doppler broadening of the two-photon transition is taken into account. We have mentioned already one limit in which (11) reduces to (8), namely, when the frequencies ω_p and ω_c are so close that one has $|\omega_p-\omega_c|/\omega_p\ll\gamma_{31}^2/\Omega_c^2$. This, however, is not really the case in our experiment, nor will it in general be the case if Ω_c is large and γ_{31} is small. We find instead that for most of our range of Ω_c the opposite inequality holds:

$$\frac{\Omega_c^2}{\gamma_{31}^2}\gg\frac{\omega_p}{|\omega_p-\omega_c|}\ . \tag{22}$$

When (22) holds, the size of the arguments z_1 and z_2 of the error functions in (11) is determined mostly by the last term inside the square root in Eq. (10) (at least when $|\Delta_1+\Delta_2|<\gamma_{31}$ and $|\Delta_1|<\omega_p\gamma_{31}/|\omega_p-\omega_c|$). This term goes as $\Omega_c^2/\Delta\omega_D\delta\omega_D$, where

$$\delta\omega_D\equiv\Delta\omega_D(\omega_p-\omega_c)/\omega_p \tag{23}$$

is the residual Doppler width of the two-photon transition. Therefore, if (22) and

$$\frac{\Omega_c^2}{\Delta\omega_D|\delta\omega_D|}\gg1 \tag{24}$$

hold, one can use the approximation (17) to simplify (11) near the two-photon resonance point. Some algebra shows that when this is done the final result (to lowest nonvanishing order in $1/|z_{1,2}|$) is once again the homogeneously broadened formula Eq. (19). Thus Eq. (19) will always hold, near $\Delta_1,\Delta_2=0$, for a sufficiently large Ω_c,

even for a Doppler-broadened medium. Again, we note that here "sufficiently large" does not mean that Ω_c has to be at all comparable to the full Doppler width; the relevant scale is set by Eq. (24) [or by (18) if $\gamma_{31} > |\delta\omega_D|$] [11].

For reference, we estimate that in our experiment the right-hand side of Eq. (24) is at most of the order of 6. This is still not quite large enough to make the use of the homogeneously broadened formulas entirely accurate and of course it gets worse for lower powers of the coupling laser. However, numerical evaluation of the general expression (11) is quite straightforward: Figure 2 shows the effect of the various broadenings and the way the homogeneously broadened limit (19) is approached at line center for a sufficiently high Rabi frequency. The solid gray line in Fig. 2 is the theoretical prediction for the absorption at line center $\Delta_1=\Delta_2=0$ as a function of the Rabi frequency and for the parameters of our experiment, for which $\delta\omega_D=-2.97$ MHz. The solid black line is the homogeneously broadened result (19), whose value at $\Omega_c=0$ has been used to normalize all the curves. The dotted line shows the prediction if the small Doppler shift of the two-photon transition is neglected, i.e., if $\delta\omega_D$ is set equal to zero [this is given by Eq. (8)]. The dashed line shows a hypothetical case with $\delta\omega_D=2.97$ MHz and all other parameters are as before.

Figure 2 indicates that for values of Ω_c smaller than those needed for (24) to hold it is actually better to have $\delta\omega_D<0$ than $\delta\omega_D>0$ or even $\delta\omega_D=0$. (This asymmetry was exhibited already, in rather extreme form, by the approximate results in [9].) The asymmetry may be understood, formally at least, by looking at the real and imaginary parts of the denominator of (5) for $\Delta_1=\Delta_2=0$:

$$= \gamma_{21} + \frac{\Omega_c^2/4}{\gamma_{31}^2+(\omega_p-\omega_c)^2 v^2/c^2} \times \left[\gamma_{31}+i(\omega_p-\omega_c)\frac{v}{c}\right] - i\omega_p\frac{v}{c} \ . \tag{25}$$

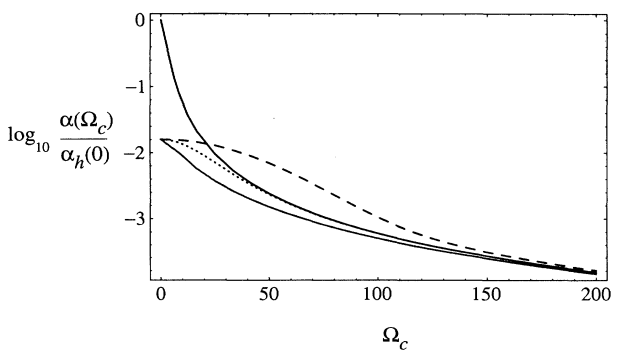

FIG. 2. Theoretical predictions for absorption coefficient α as a function of Rabi frequency Ω_c, on resonance at line center ($\Delta_1=\Delta_2=0$). $\gamma_{21}=3$ MHz and $\gamma_{31}=0.5$ MHz. Solid black line, α_h, the homogeneously broadened case ($\Delta\omega_D=\delta\omega_D=0$); solid gray line, $\Delta\omega_D=540$ MHz and $\delta\omega_D=-2.97$ MHz; dashed line, $\Delta\omega_D=540$ MHz and $\delta\omega_D=2.97$ MHz; dotted line, $\Delta\omega_D=540$ MHz and $\delta\omega_D=0$.

If $\delta\omega_D<0$, that means we have $\omega_p<\omega_c$, and in this case the term proportional to $(\omega_p-\omega_c)v/c$ in (25) will add up to the other imaginary part $-\omega_p v/c$; this makes the imaginary part of (5) smaller, overall, for any velocity v, than in the opposite case, with $\delta\omega_D>0$ (i.e., $\omega_p>\omega_c$), where the term proportional to $(\omega_p-\omega_c)v/c$ partly cancels the $-\omega_p v/c$ term.

Finally, we must consider briefly, for the purpose of comparison with the experiments, the effect of a finite laser linewidth. A simple way to account for this is to assume that the experimental curves will be proportional to the convolution of (11) with the laser line shapes, the relevant variables being the frequencies ω_c and ω_p [12]. If the line shapes are Lorentzian, one can take advantage of the simple result

$$\int_{-\infty}^{\infty} \frac{f(x)}{(x-x_0)^2+\gamma^2}dx = \frac{\pi}{\gamma} f(x_0+i\gamma) \ , \tag{26}$$

valid for any function $f(x)$ analytic in the upper half plane (including infinity). It can be shown that $\chi(v)$ in Eq. (5) is such a function of ω_c and ω_p, provided that the integral over velocities is truncated so as not to allow speeds greater than that of light (of course, such a truncation has a negligible effect in the final result). Then the result of the convolution, apart from an overall multiplicative factor, is to replace ω_p everywhere by $\omega_p^0+i\gamma_p$, where ω_p^0 and γ_p are the nominal frequency and the half linewidth of the probe laser, respectively, and similarly to replace ω_c by $\omega_c^0+i\gamma_c$. This replacement has negligible consequences, because of the smallness of $\gamma_{p,c}$ compared to ω, everywhere except in the detunings Δ_1 and Δ_2. Inspection of (10)–(12) then shows that all that is necessary is to change the effective linewidths

$$\gamma_{21}\to\gamma_{21}+\gamma_p, \quad \gamma_{31}\to\gamma_{31}+\gamma_p+\gamma_c \ . \tag{27}$$

For our experiment, $\gamma_p\simeq\gamma_c\simeq 2.5$ MHz. It should be kept in mind that this very simple approach will not hold, in general, if the laser line shape is not Lorentzian.

The replacement (27) indicates that a large laser linewidth will reduce the observed transparency because of the sensitivity of our equations to the effective value of γ_{31}. Figure 3 shows the theoretical prediction for

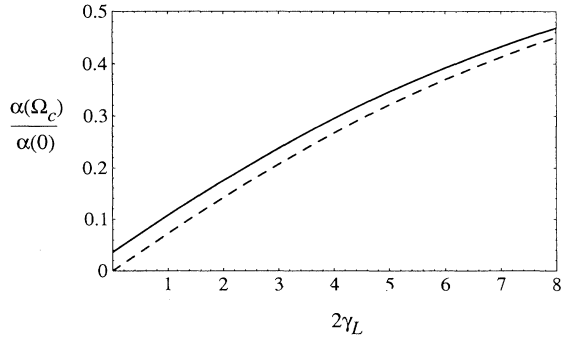

FIG. 3. Theoretical prediction for the absorption coefficient at line center ($\Delta_1=\Delta_2=0$) as a function of laser linewidth. Solid line, $\gamma_{21}=3$ MHz, $\gamma_{31}=0.5$ MHz, $\Omega_c=92$ MHz, $\Delta\omega_D=540$ MHz, and $\delta\omega_D=-2.97$ MHz; dashed line, the limit $\gamma_{31}=0$ (other parameters are the same).

$\alpha(\Omega_c)/\alpha(0)$ as a function of the laser full linewidth $2\gamma_L$ (assuming $\gamma_p \simeq \gamma_c \simeq \gamma_L$), at line center ($\Delta_1=\Delta_2=0$), and for the parameters in our experiment (in particular, we use the inferred effective Rabi frequency $\Omega_c \simeq 92$ MHz; see Sec. III). The dashed line illustrates what one might observe instead if the third level had an infinite lifetime, i.e., if $\gamma_{31}=0$ instead of $\simeq 0.5$ MHz. Clearly, at $2\gamma_L=5$ MHz we are mostly limited by the finite laser linewidth.

D. Summary

The main points of the foregoing analysis may be summarized as follows.

Assume an inhomogeneously broadened medium ($\Delta\omega_D \gg \gamma_{31},\gamma_{21}$), under conditions of one- and two-photon resonances, for simplicity ($\Delta_1=\Delta_2=0$). Also assume $\gamma_{31}<\gamma_{21}$ since there is no apparent advantage in coupling a long-lived transition to a short-lived one. (In all that follows, from the point of view of what may be observed in a particular experiment, γ_{31} and γ_{21} may need to be augmented by the laser linewidth as necessary.) If a "Doppler-free" arrangement is used (counterpropagating beams for the cascade system, copropagating for the Λ system), then let $|\delta\omega_D|$ be the residual Doppler width of the two-photon transition [see Eq. (23)]. Two regimes are then possible.

(i) If the level spacings are matched so that $|\delta\omega_D| \ll \gamma_{31}$, the condition to observe a large reduction in absorption on resonance is given by Eq. (18). This is analogous to the homogeneously broadened case [Eq. (21)], except that the width $\Delta\omega_D$ has replaced the original homogeneous width (radiative or collisional) γ_{21} of the probe transition. Still, Eq. (18) shows that it is not necessary for the pump Rabi frequency to exceed the Doppler width and that in principle arbitrarily small absorption can be achieved even for a small Ω_c, provided only that γ_{31} be small enough (this also parallels the homogeneously broadened case [7]). The difficulty in achieving this Doppler-free regime is finding levels with almost identical separations. This may be especially hard in the cascade configuration (although our experimental system actually comes pretty close), but may be not as difficult for the Λ systems, where $|1\rangle$ and $|3\rangle$ may just be different magnetic or hyperfine sublevels.

(ii) For a small enough γ_{31} or a large enough $|\delta\omega_D|$ that the two-photon transition may not be regarded as Doppler-free (in particular, when $|\delta\omega_D| \geq \gamma_{31}$), the condition for a substantial reduction of absorption on resonance is Eq. (24) instead [at least for $\delta\omega_D>0$; see (iv) below for the other case]. This may still be achieved for an Ω_c considerably smaller than the full Doppler width, if $|\delta\omega_D|$ can be made small enough.

(iii) In either case, the homogeneously broadened formulas are recovered, near resonance, for a sufficiently large Ω_c. The condition for this "power broadening" to occur is again (18) or (24) (whichever is largest).

(iv) For values of Ω_c too small to satisfy (24), it is advantageous (from the point of view of reducing the absorption on resonance) to have a negative $\delta\omega_D$ rather than a positive or even zero (completely Doppler-free) value. When inhomogeneous broadening is important, therefore, one should look for systems where $\omega_{32}>\omega_{21}$. (Note that for the Λ-type systems this means that, ideally, the coupling level $|3\rangle$ should be located somewhat below the "ground" level $|1\rangle$.) Our numerical calculations suggest that it is generally better to have $-\delta\omega_D$ as large as possible, especially for small Ω_c; if Ω_c is already large enough to satisfy (18), we find that there is little additional benefit in making $-\delta\omega_D$ much greater than a few times γ_{31}.

III. EXPERIMENTAL RESULTS

In this section the theoretical treatment will be compared with our experimental results. The experiments were done with rubidium atoms in a vapor cell at room temperature [4]. The pumping laser of wavelength 775.8 nm couples the upper transition from state $5P_{3/2}$, $F=4$ (state $|2\rangle$) to state $5D_{5/2}$, $F=5$ (state $|3\rangle$) and the probe laser of wavelength 780.0 nm couples one hyperfine transition of state $5S_{1/2}$, $F=3$ (state $|1\rangle$) to state $5P_{3/2}$, $F=4$ (state $|2\rangle$), which is the Rb D2 line. This three-level ladder-type system is exactly the one that we used in the theoretical model described in the preceding section. The condition $\omega_c-\omega_p>0$ is satisfied in this system, which is favorable for EIT as discussed earlier. The natural linewidth Γ_2 of the rubidium $D2$ line is about 6.0 MHz and the natural linewidth Γ_3 of the transition between the states $5P_{3/2}$ and $5D_{5/2}$ is about 0.97 MHz. The Doppler width at room temperature is about 540 MHz.

The experimental arrangement is shown in Fig. 4. The probe and pumping beams are orthogonally polarized and they propagate in opposite directions through a 76.0-mm-long rubidium vapor cell kept at room temperature (around 21 °C–22 °C). Both diode lasers (DL1 and DL2) are frequency and temperature stabilized to give a linewidth of about 5 MHz, which is the Schwalow-Townes limit. The pumping laser (DL2) is a laser diode at wavelength 775.8 nm with maximum output power of 20 mW at the cell position. This pumping beam is focused by a 10-cm lens onto the cell. The pumping intensity at the beam waist is estimated to be 250 W/cm^2. The probe laser (DL1) is a laser diode at wavelength of 780.0 nm. To get a good beam profile, a 0.5-mm aperture is

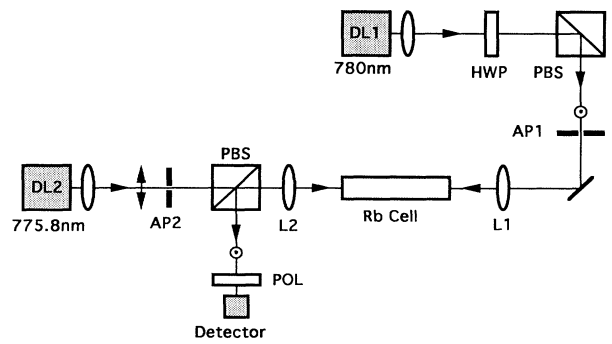

FIG. 4. Experimental arrangement. DL1 and DL2, diode lasers; PBS, polarizing cube beam splitter; AP1 and AP2, apertures; L1 and L2, lenses; HWP, half wave plate; POL, polarizer.

used. The signal beam is also focused by a 10-cm lens onto the cell to match the pumping beam. A polarizer is used in front of the detector to eliminate the scattered light from the strong pumping beam by the windows of the cell.

When the pumping beam is blocked, typical absorption curves of the probed transition for two-level atoms are recorded (we concentrate only on one absorption line of ^{85}Rb between $5S_{1/2}$, $F=3$ and $5P_{3/2}$), as shown in Fig. 5(a). The maximum absorption coefficient at the center frequency of the Doppler-broadened line is measured to be $\alpha \approx 8.2\times10^{-2}$ cm^{-1}. The room temperature was measured to be $T=21.0$°C during the experiment. With pumping Rabi frequency set to zero, Eq. (11) for the absorption part is plotted (gray curve) together with the experimental curve (dark solid curve) with a laser linewidth of 5.0 MHz and a Doppler width of 540 MHz. The atomic decay rate Γ_2 is taken to be 6.0 MHz and Γ_3 to be 0.97 MHz. When the pumping beam is applied and tuned to the resonance frequency $\Delta_2=0$, a narrow dip at the center of the absorption profile appears, as shown in Fig. 5(b). Equation (11) for the absorption part is plotted (gray curve) together with the experimental results (dark solid curve). In this theoretical plot, all the parameters are the same as used in Fig. 5(a), except for the nonzero Rabi frequency $\Omega_c=92$ MHz.

The only adjustable parameter in our theory is the pumping Rabi frequency Ω_c. In our experiment, two major factors contribute to the uncertainty in determining the Rabi frequency Ω_c for the pumping beam. One is the tight focus of the pumping beam. The output of the diode laser is an elliptical shape with the ratio of two major axes of about 3:1. The Rayleigh lengths of the two axes are about 3.2 and 31.0 mm, respectively. Since the cell is about 76 mm long, the field is nonuniform inside the atomic medium. Hence it is very difficult to convert the pumping power into an effective Rabi frequency with high accuracy. In our current theoretical treatment, the change in the pumping intensity along the cell and the spatial shape in the radial direction (Gaussian beam profile) have not been taken into account. Additionally, the mode matching of the probe and pumping beams are not perfect. Due to the experimental arrangement, the probe beam is comparable to the pumping beam in spatial size. With the tight focusing, exact mode matching efficiency is hard to determine, which contributes to the uncertainty of the effective pumping Rabi frequency. Other than the uncertainty in pumping Rabi frequency, we have not considered the effect due to hyperfine structures on the excited states $5P_{3/2}$ (state $|2\rangle$) and $5D_{5/2}$ (state $|3\rangle$). The closest hyperfine structure separation in state $5P_{3/2}$ is about 121 MHz ($F=3$ and 4), which will have little effect on our experiment. However, the separation between the closest hyperfine structures in state $5D_{5/2}$ is 9.4 MHz ($F=4$ and 5), which is within the linewidth of the resonance dip in Fig. 5(b). We attribute the broadening of the dip to the effect of hyperfine structures in state $5D_{5/2}$. The experimental results and the theoretical curves seem to agree very well in Figs. 5(a) and 5(b).

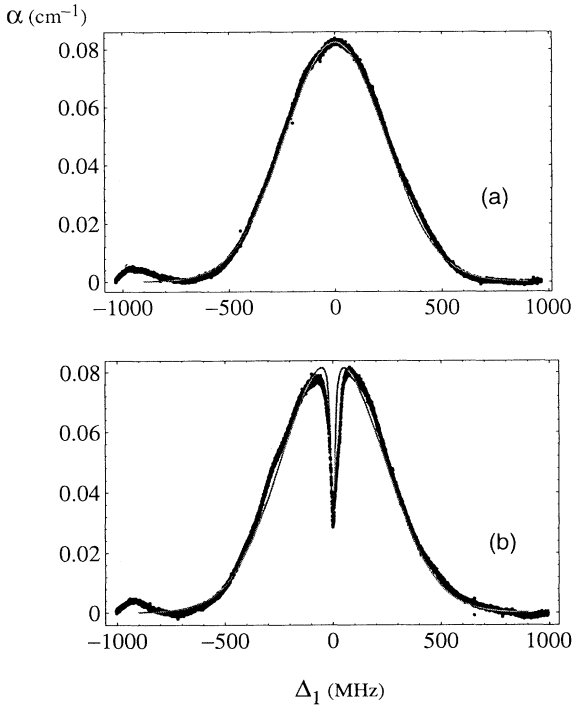

FIG. 5. Absorption coefficient α as a function or probe detuning Δ_1. Heavy black curve, experiment; gray curve, theory. (a) No coupling laser. (b) Coupling laser on resonance $\Delta_2=0$. The theoretical parameters are $\gamma_{21}=3$ MHz, $\gamma_{31}=0.5$ MHz, $\Omega_c=92$ MHz, $\Delta\omega_D=540$ MHz, $\delta\omega_D=-2.97$ MHz, and laser (half) linewidth $\gamma_c=\gamma_p=2.5$ MHz.

From Fig. 5(b), a new absorption coefficient $\alpha \approx 2.90\times10^{-2}$ cm^{-1} is obtained at the center frequency. This change in absorption at resonance gives an absorption reduction of 64.4%. As discussed in Sec. II, this reduction in absorption is the result of atomic coherence induced by the pumping field. The current limiting factor in absorption reduction is the laser linewidth. From Fig. 3 one can see that, by simply reducing the laser linewidth to 0.5 MHz, we could, in principle, achieve an absorption reduction of 92.5%.

When the pumping beam is tuned off resonance ($\Delta_2=-320$ MHz), a dispersionlike structure appears at the side of the Doppler-broadened absorption curve [Fig. 6(a)] as a result of contributions from absorption reduction due to atomic coherence and enhancement due to two-photon absorption. Figure 6(b) is the absorption curve when the pumping frequency is tuned far from resonance ($\Delta_2=-800$ MHz). The absorption peak is due to two-photon absorption from state $|1\rangle$ to state $|3\rangle$. Again, theoretical results from Eq. (11) for the absorption part are plotted (gray curves) with the experimental data (dark solid curves) in these two curves. The parameters used in the theoretical plots are the same as in Figs. 5(a) and 5(b), except for the detuning of the pumping frequency Δ_2. In particular, the same effective Rabi frequency is used in Figs. 5(b), 6(a), and 6(b).

We have measured the change in absorption coefficient with the pumping power for both on-resonance pumping

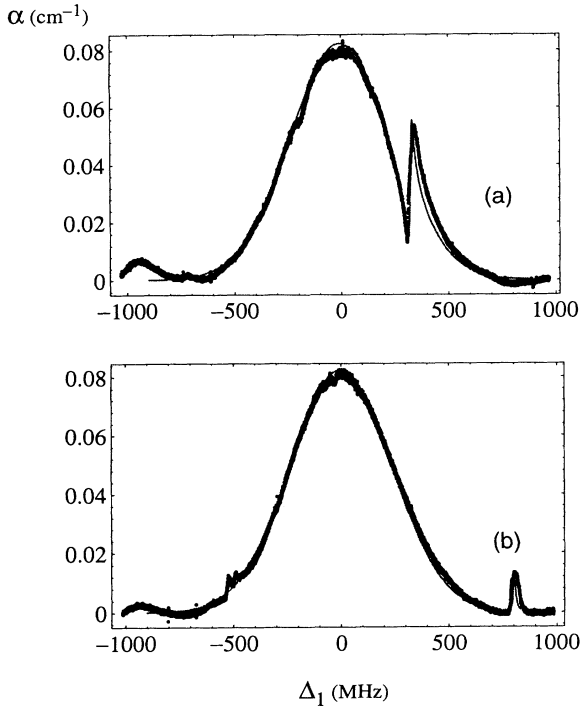

FIG. 6. Same as Fig. 5 for a detuned coupling beam. (a) $\Delta_2=-320$ MHz. (b) $\Delta_2=-800$ MHz. All other parameters are the same as in Fig. 5.

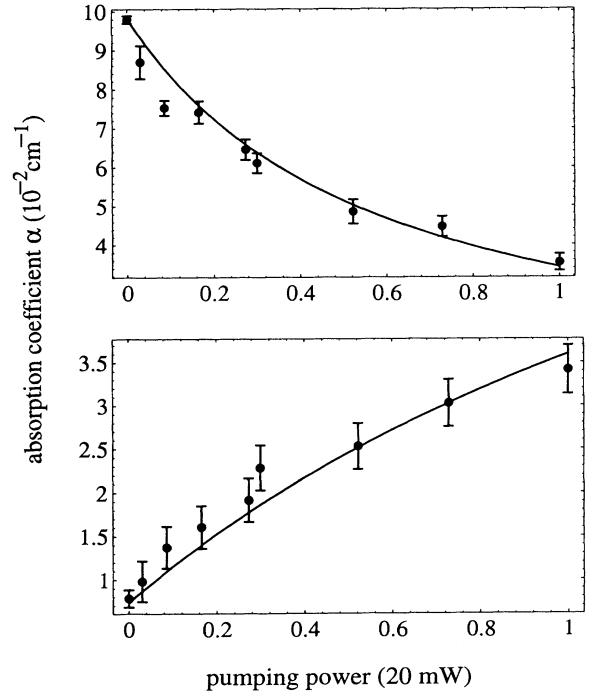

FIG. 7. Absorption coefficient versus pumping power for (a) $\Delta_2=\Delta_1=0$ and (b) $\Delta_2=-550$ MHz and $\Delta_1\simeq 550$ MHz (the two-photon absorption peak is slightly shifted from $\Delta_1=-\Delta_2$). Solid line, theoretical prediction [the parameters are the same as in Figs. 5 and 6, with the abscissa equal to Ω_c^2 in units of (92 MHz)^2].

[Fig. 7(a)] and off-resonance pumping [Fig. 7(b)]. In the on-resonance pumping case ($\Delta_2=0$), the absorption coefficient is reduced at center frequency of the probe beam as the pumping power increases. This absorption reduction is due to atomic coherence induced by the pumping beam. Equation (11) for the absorption part is plotted together with experimental data in Fig. 7(a). These measurements were done on a different day and the temperature measured was $T=22.5$ °C. The new absorption coefficient in the absence of the pumping beam is $\alpha\approx 9.8\times 10^{-2}$ cm^{-1}. The pumping power was measured experimentally for each point. In the theoretical treatment, however, the Rabi frequency Ω_c is the parameter. Therefore, the only adjustable parameter is the conversion from pumping power to Rabi frequency Ω_c as stated earlier. The parameters used for the theoretical plot are the same as those used in Figs. 5 and 6. The agreement is quite remarkable. We also measured the increase in absorption due to two-photon absorption when the pumping beam is -550 MHz off resonance with the $|2\rangle\rightarrow|3\rangle$ transition ($\Delta_2=-550$ MHz). Equation (11) for the absorption part is again plotted with the experimental data in Fig. 7(b). The experimental curve seems to bend more than the theoretical one. We believe that this disagreement is due to our neglecting the spatial variation of the pumping beam inside the vapor cell in our theoretical treatment.

IV. CONCLUSION

In this paper, a simple theoretical model was developed to understand an experiment done in a three-level ladder-type system in rubidium atoms. Results of the theoretical analysis are summarized in Sec. II D.

We have also presented experimental measurements of the absorption of a three-level ladder-type atomic system in rubidium together with the theoretical results. From our measurement, the absorption is reduced by 64.4% for the probe beam at its resonance frequency when the pumping field is on resonance with the upper transition. The absorption on resonance can be further reduced if we reduce the linewidth of the laser diodes and eventually the reduction will be limited by the finite linewidth of the upper state $|3\rangle$. In the limit when the laser linewidth and the decay rate of state $|3\rangle$ go to zero, one can expect perfect transmission in an otherwise absorptive atomic medium by using a pumping laser. This effect (reduced absorption in a medium) can find many applications in nonlinear optics and optoelectronic devices.

This measurement has a high-frequency resolution with low pumping power and provides a meeting ground for the experimental results and theoretical calculations. Our simple theoretical model gives results in remarkable agreement with the experimental measurement. We believe that the simple theoretical calculation is also useful in clarifying the mechanism of EIT.

ACKNOWLEDGMENT

M. X. acknowledges partial support from the National Science Foundation through Grant No. PHY9221718.

[1] A. Imamoğlu and S. E. Harris, Opt. Lett. **14**, 1344 (1989).

[2] Some other theoretical proposals for lasers without inversion are S. E. Harris, Phys. Rev. Lett. **62**, 1033 (1989); M. O. Scully, S.-Y. Zhu, and A. Gavrielides, *ibid.* **62**, 2813 (1989). For recent experiments, see E. Fry *et al.*, Phys. Rev. Lett. **70**, 3235 (1993); W. E. Van der Veer *et al.*, *ibid.* **70**, 3243 (1993); A. Nottelmann *et al.*, *ibid.* **70**, 1783 (1993). For further references, see the review articles by O. Kocharovskaya, Phys. Rep. **219**, 175 (1992); M. O. Scully, *ibid.* **219**, 191 (1992).

[3] M. O. Scully, Phys. Rev. Lett. **67**, 1855 (1991); M. O. Scully and M. Fleischhauer, *ibid.* **69**, 1360 (1992); U. Rathe *et al.*, Phys. Rev. A **47**, 4994 (1993); S. E. Harris, J. E. Field, and A. Kasapi, *ibid.* **46**, R29 (1992); S. E. Harris, J. E. Field, and A. Imamoğlu, Phys. Rev. Lett. **64**, 1107 (1990).

[4] M. Xiao, Y. Li, S. Jin, and J. Gea-Banacloche, Phys. Rev. Lett. (to be published).

[5] For previous experiments, see K.-J. Boller, A. Imamoğlu, and S. E. Harris, Phys. Rev. Lett. **66**, 2593 (1991); J. E. Field, K. H. Hahn, and S. E. Harris, *ibid.* **67**, 3062 (1991); K. Hakuta, L. Marmet, and B. P. Stoicheff, *ibid.* **66**, 596 (1991); G. Z. Zhang, K. Hakuta, and B. P. Stoicheff, *ibid.* **71**, 3099 (1993).

[6] M. Sargent III, M. O. Scully, and W. E. Lamb, Jr., *Laser Physics* (Addison-Wesley, Reading, MA, 1974).

[7] M. Fleischhauer, C. H. Keitel, L. M. Narducci, M. O. Scully, S.-Y. Zhu, and M. S. Zubairy, Opt. Commun. **94**, 599 (1992).

[8] *Handbook of Mathematical Functions,* Natl. Bur. Stand. Appl. Math. Ser. No. 55, edited by M. Abramowitz and I. A. Stegun (U.S. GPO, Washington, DC, 1965), Chap. 7, Eqs. 7.1.3 and 7.1.4.

[9] Th. Hänsch and P. Toschek, Z. Phys. **236**, 213 (1970). For a related experiment, see T. Hänsch, R. Keil, A. Schabert, Ch. Schmeltzer, and P. Toschek, *ibid.* **226**, 293 (1969).

[10] A. Imamoğlu, Phys. Rev. A **40**, 2835 (1989).

[11] Conditions (18) and (24) for the Doppler broadening to be negligible have also been derived, in the context of an EIT atomic magnetometer, by M. Fleischhauer and M. O. Scully, Phys. Rev. A **49**, 1973 (1994).

[12] For the homogeneously broadened case, our results reduce to those obtained recently by S. Sultana and M. S. Zubairy, Phys. Rev. A **49**, 438 (1994), from a somewhat more sophisticated approach.